Celal Bayar University Journal of Science

Effective Reduction of Graphene Oxide via *Lactococcus lactis*

Guldem Utkan[1]*

[1]Marmara University, Faculty of Engineering, Chemical Engineering Department, Göztepe Kampüsü, 34722 Kadıköy, Istanbul
*guldem.utkan@marmara.edu.tr
*Orcid: 0000-0002-5522-9940

Received: 27 March 2020
Accepted: 15 June 2020
DOI: 10.18466/cbayarfbe.710338

Abstract

In this study, bacteria *Lactococcus lactis* was employed as a bioreducing agent for ecofriendly and economical production of reduced graphene oxide at room temperature. Characterizations have showed that highly reduced graphene oxide was produced in mild conditions. Exfoliation by *Lactococcus lactis* has been succeeded to produce single or few layer reduced graphene oxide. Decrease in ratio of I_D/I_G from 2.15 to 0.97 calculated from Raman spectrum, decrease and/or disappearance of characteristic peaks of oxygen functional groups from FTIR, and changes observed in 2θ characteristic peak values at XRD spectrum have confirmed the reduction success of *Lactococcus lactis*. These results have indicated that *Lactococcus lactis* biomass could be employed as a new reductant to prevent the use of harmful chemicals and harsh conditions for reduced graphene oxide generation having high stability.

Keywords: Graphene, *Lactoccoccus*, microbial reduction, 2D material.

1. Introduction

In recent years, extensive potential applications of graphene derived materials in particular graphene oxide (GO), reduced graphene oxide (RGO) has attracted attentions [1]. With the increase in graphene commercialization, the more need for finding ecofriendly production methods [2] have been appeared. Most of the methods generally start with GO production from graphite and reduction processes apply to produce RGO. Various techniques for reduction, i.e. thermally, chemically etc., has been reported for production of reduced GOs. Chemical reduction is the most widely used method, however, there have been records for the use of hazardous and harmful chemical substances, i.e. hydrazine, sodium borohydride etc., for efficient reduction of GO. On the other hand, vitamin C, bovine serum albumin, ginseng, green tea, and bacteria have recently been studied as green reduction agents [3]. These agents have provided environmentally friendly GO reduction paths [4] as an alternative.

Bacteria may extract some molecules from their environment to live. They convert these molecules into materials that can be used by the oxidation-reduction mechanism for their cellular cycles [5]. There are studies using the general redox cycle performed by bacteria such as *Shewanella* [6], *Bacillus subtilis* [7], *Escherichia coli* [4], and other microorganisms [8-13] in GO reduction. It should be noted that the mechanisms involved in the reaction that determine the capacity to hydrolyze oxygen groups in GO depend on the bacterial cell structure. In one study, *Shewanella* [6] was used to reduce GO. Here, it is reported that electron exchange is provided by the mechanism where heme-type proteins are used for reduction [14]. In another study [7], it was stated that the properties of the final material to be obtained in accordance with the application to be used can be selected by a method according to the type of bacteria to be used in reducing GO. It was also suggested that in bacterial reduction processes the efficacy could be improved by simultaneous use of different bacteria. Based on the findings of Zhang, Raveendran et al [8] manage to reduce GO using extremophile bacteria to obtain graphene with excellent conductive properties. Utkan et al [15] used *Lactobacillus plantarum* (*L. plantarum*) biomass for the reduction of GO and a few layer of RGO without agglomeration was obtained.

There are many different reducing agents used for reduction of GO as mentioned above Each of the

reducers affected the structure of the RGO, in other words, it gave different structural properties than GO [3]. These structural differences has been characterized as differences in C/O ratio as shown in Table 1 as well as the change in intensity ratio (I_D/I_G) between graphene defects/the surface disorder and the graphitic composition of the materials as given in Table 2.

Table 1. C/O ratio of RGO after different reduction process.

Reducing agents	C/O Ratio	Reference
Hydroxylamine	9.7	[16]
L ascorbic acid	5.7	[17]
Tea solution	3.1	[18]
Yeast	5.9	[19]
Shewanella	3.1	[6]
Azotobacter chroococcum	4.18	[9]
Lactococcus plantarum	3.3	[15]

Table 2. I_D/I_G ratio of GO and RGO with different reducing agents.

Reducing agents	I_D/I_G for GO	I_D/I_G for rGO	Reference
Baking Soda	1.47	1.37	[20]
E-coli	1.37	097	[21]
Vitamin C (L-Ascorbic acid	0.95	1.2	[22]
Tanin	0.97	1.18	[23]
Yeast	0.80	1.44	[19]
Lactobacillus plantarum	0.94	0.92	[15]
Shewanella onediens	085	1	[6]
Mixed bacteria	0.9	1.5	[7]
Rhizopus oryzae	0.97	1.17	[12]
Bacillus marisflavi	1.4	1.7	[13]

In this study, first time reduction of GO by *Lactoccocus lactis* DSMZ 20481 (*L. lactis*) cells under aerobic culture was obtained. It was demonstrated that reduction capacity of the microorganisms was considerable with respect to other microorganisms reported [6, 15, 21]. Single/a few layer graphene structures were obtained successfully. Produced RGO has showed different physical properties compared to the one obtained in our previous study with *L. plantarum* [15]. Compared to conventional methods, the microbial reduction used in this study is environmentally friendly and simple method to be employed for the production of large amount of graphene.

2.1. Experimental

2.1.1. Materials

Graphite, including graphitic carbon with 92%, in powder form was supplied from Syrah Resources (Australia). All chemicals, potassium permanganate ($KMnO_4$), nitric acid (HNO_3), sulphuric acid (H_2SO_4, 98%), hydrogen peroxide (H_2O_2, 30%), hydrochloric acid (HCl, 36%), ethanol were supplied by Sigma-Aldrich (USA) and used directly. Solutions were prepared by deionized water. *Lactococcus lactis* (20481) were provided from the German Collection of Microorganisms and Cell Cultures GmbH (DSMZ) and cultured in DSMZ medium no 53 medium.

2.1.2. Preparation of bacterial biomass

Precultures and bacterial biomass was prepared according to procedure in Utkan et al [15] in medium DSMZ 53 and phosphate-buffered saline (pH 7.2) was used for washing the harvested cells. Wet cells around 200 mg were obtained.

2.2.3. Graphene oxide preparation

For GO preparation and purification, Utkan et al [15] procedure based on modified Hummer's method [2] was followed. 6 mg/ml dark brown GO dispersion was obtained after 2 hr sonification.

2.1.3. Reduction of graphene oxide

Dilute, 0.5 mg/ml, GO dispersion was added to 200 mg of *L. lactis* biomass and incubated at 30°C. A static culture was applied for 3-4 days and black precipitate (RGO) was obtained. After 5 min sonification, bacteria removal was accomplished by 10,000 rpm/min, 10 min centrifugation. The black pellet (RGO) was suspended in water and successive 80% ethanol and 1N HCl washings were applied [5]. Lyophilized black precipitate was named as *L. lactis* reduced graphene oxide (LLRGO).

2.1.4. Characterization

Fourier transformed infrared spectroscopy (FTIR) (Shimadzu IR Prestige 21) was employed for chemical characterizations. Pellets of samples were prepared in potassium bromide (KBr). Microconfocal Raman spectra (Renishaw Invia Raman Microprobe with argon ion laser 532 nm) were used for characterization of GO and RGO samples and recorded from 200 to 3000 cm^{-1}. X-ray diffraction (XRD, Rigaku MinFlex, D/max 2550-PC) with Cu Ka radiation (λ=0.15406nm) was employed with scanning rate of 2º min^{-1}(2θ=5-90º).

Thermogravimetric analysis (TGA) (TA Instrument Thermogravimetric Analyzer Q50) of GO and RGO was carried out under nitrogen. 5°C/min heating rate up to 600 °C was applied to the samples.

Celal Bayar University Journal of Science
Volume 16, Issue 2, 2020, p 155-160
Doi: 10.18466/cbayarfbe.710338

High resolution transmission electron microscopy (HRTEM) (JEOL JEM 2100 HRTEM) with 200 kV was used for characterization of morphology of the samples. Samples were prepared on 200 mesh copper grids and CCD cameras were employed for taking images. An atomic force microscopy (AFM) (XE-150, non-contact mode; Park systems) with a stylus profiler (P-6; KLA Tencor, Milpitas) was used to determine nanostructure of the samples.

3. Results and Discussion

3.1. Structural Characterization

3.1.1. FTIR

Chemical structures were determined by FTIR. In Figure 1, characteristic peaks of GO were C-O stretching at 1111 cm^{-1}, C-O-C bending at 1219 cm^{-1}, C-OH stretching at1404 cm^{-1}, C=O stretching at 1643 cm^{-1} and O-H stretching vibration of C-OH groups and water at 3441 cm^{-1} were observed. When the RGO spectrum were considered, reduction by *L. lactis* biomass was observed as removal and/or reduction of functional group peaks existing on GO. In RGO spectrum, the peaks at 1111, 1219 cm^{-1} were disappeared and 1643, 3441 cm^{-1} was decreased significantly. This result is an evidence of effective reduction of oxygen groups existing on GO. Removal of some peaks indicated that corresponding functional groups were used by *L. lactis* by their oxidation-reduction mechanism however, reduced peaks were still on RGO with weaker intensity which shows the existence of residual oxygen containing functionalities. It means that *L. lactis* was very effective to remove some of the functionalities more than the others [11, 15]. It should be also noted that the carbonyl peak on GO at 1643 cm^{-1} overlapped with sp^2 lattice at 1639 cm^{-1} which corresponds to graphene sheet aromatic ring C=C peak. The results obtained by FTIR analysis are in agreement with literature [3].

3.1.2 Raman Analysis

The Raman spectra of graphene shows the appearance in Figure 2, D peaks at 1350 and G peaks at 1580 cm-1 confirm the lattice distortions in GO. The D band shows the surface disorder and graphene defects and the G band expresses the materials' graphitic composition. Intensity ratio (I_D/I_G) between D and G band is used for distinguishing RGO and GO and it is giving information about the disorder grade of graphene. I_D/I_G ratio either decreased or increased with respect to reducing agent used in literature as seen in Table 2. This is explained by occurrence of two different regime: the high defect density regime and the low defect density regime. At high defect density, the ratio starts to fall with increment of defect density and forms more amorphous carbon texture graphene structure. At low defect density regime, the ratio starts to increase, and more crystalline structure obtained [3].

In our case, ratio of peak intensity (I_D/I_G) which represents defect ratio coming from oxygenation of graphitic carbons are about 2.15 for GO and 0.97 for RGO. It meant that chemical oxidation produced a lot of defects on sp^2 region and graphitic domain decreased but applying reduction process with removal of functional groups recovered the sp^2 graphitic domain significantly.

Decrease of I_D/I_G ratio has corresponded to size decrease in domain of sp^2 that means decrease in edge defects in GO. Similar trend, decrease in intensity ratio from GO to RGO, was observed in literature with different reducing agents, for example, for baking soda from 1.47 to 1.37 [20], for *L. plantarum* from 0.94 to 0.92 [15], and for *E coli* from 1.37 to 0.97 [21]. But, none of them have high recovery of sp^2 domain as obtained with *L. lactis*. All carbon materials having sp^2 domains give G band, and this peak comes from first order Raman scattering of C-C bond. After oxygenation of graphite to GO, sp^3 domains form. Oxygenation moves G band to a higher wave number. During the oxygenation, formation of defects reduces sp^2 domain size which has broadened D band in GO.

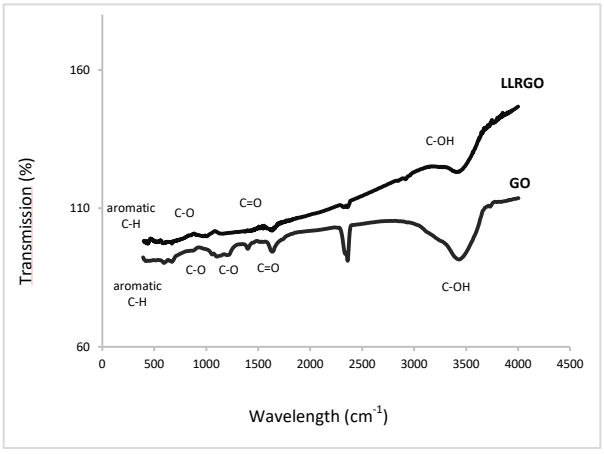

Figure 1. Chemical structure of GO and LLRGO by FTIR.

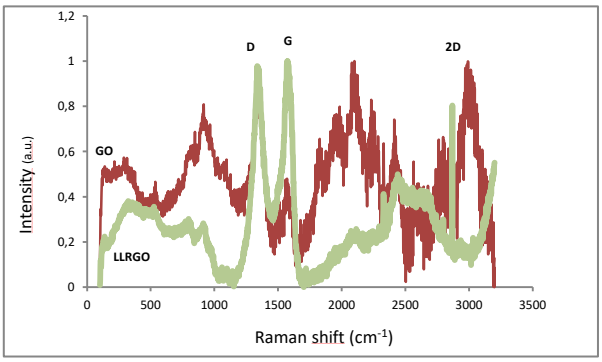

Figure 2. Raman spectrum of GO and LLRGO.

3.1.3 XRD

Celal Bayar University Journal of Science
Volume 16, Issue 2, 2020, p 155-160
Doi: 10.18466/cbayarfbe.710338

Graphite has highly organized layer structure and XRD gives a single very sharp 2θ peak at around 26.24°. This peak belongs to (002) plane. The distance between layers has been calculated as 0.34 nm for graphite by using Braggs' law [3]. When graphite oxidized, GO forms, and at this point the graphite sharp peak disappears, however, a new plane along (001) appears at around 10°. In figure 3, (001) plane for GO obtained was at around 9.98°. From this peak, distance between layers was calculated as 0.89 nm according to Braggs' law [3]. Higher interlayer spacing was observed for GO compared to graphite (0.34 nm, 2θ=26.24°), which shows that oxygen functional groups and water molecules existing between layers opened up well the distances between layers. This expected result has showed that graphite has almost had complete oxidation. It was also observed that there is a very small broad peak around 25.9° in Figure 3, it was speculated that this peak came from un-oxidized part of the graphite.

After reduction, XRD pattern of obtained RGO, in Figure 3, has showed that GO peak along (001) plane moved to 2θ =11.35°. In the same way, graphitic (002) plane at 2θ = 23°–26° has been appeared as small wide peak. The peak of (001) orientation plane seen at 2θ =11.35° comes from unreduced oxygenated part of RGO and it has 0.78 nm distance between layers. This interlayer distance is either due to restacking of RGO layers or with the sacrification of groups containing oxygen functionality. The small wide peaks in the range of 23°–26° represented the disposal of oxygen functional groups by this way RGO having graphitic carbon was observed as few layers RGO sheets formation. It was speculated that the formation of few layer RGO with interlayer distance of 0.78 nm may be resulted from restacking of RGO formed with 0.34 nm interlayer distance. Thus, decrease in distance between layers has been approved by the dispose of oxygen groups [3]. These results are in agreement with literature [24].

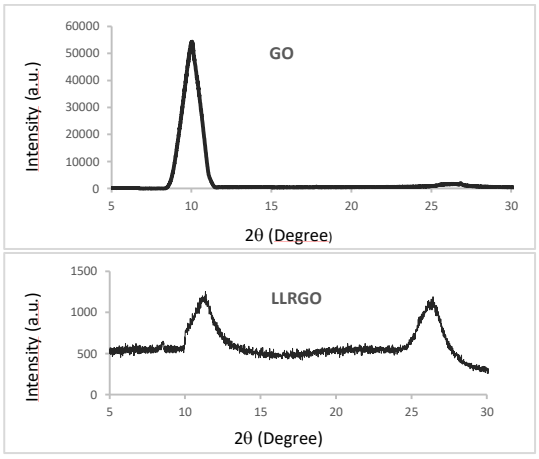

Figure 3. GO and LLRGO XRD pattern.

3.2. Thermal Analysis
3.3.2.1 TGA

Thermal stability of samples was evaluated by TGA as seen in Figure 4. It was observed that there were two weight loss steps in the range of 25-300°C for both GO and RGO. These meaningful weight losses of 48% and 23% for temperatures are in the range of 25-168°C and 168-300°C for GO. For RGO, 11% weight loss for 25-300°C and 18% weight loss for 25-300°C were determined. The first step has been grounded to the hydrophilicity of GO and the elimination of adsorbed water molecules. The second one has been connected to both release of steam and gases such as CO_2 and CO that comes from decomposition of functional groups. At this temperature range, 25-300°C, GO lost almost 71% of weight, however, RGO lost only 29% of weight which means as reduction progressed, oxygen functional groups decomposition was resulted in as minimal weight loss in RGO. When high temperature region (>300°C) in Figure 4 was examined, continuous, but slow, weight losses in both GO and RGO were observed. The weight loss percentages at 450°C reached to 94% for GO and 40% for RGO. This thermal behavior has been explained by dissipation of more stable functional groups and burn of carbon skeleton.

Similar thermal behavior for RGO has been reported in literature [25, 26, 28].

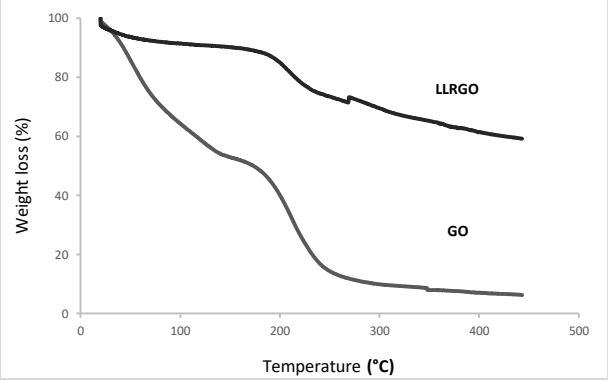

Figure 4. Thermal stability of GO and LLRGO by thermogravimetric analysis.

3.3 Topographical Analysis
3.3.1 AFM

Surface topographical image of *L. lactis* reduced graphene oxide is given in Figure 5. Micrograph has been taken from scanned area of 1 µm X 1 µm. Surface roughnesses were observed as optical contrast in the AFM image where the higher layers give whitish color from their reflections. When this image considered together with TEM image (Figure 6), it is attributed to the existence of wrinkles. It was thought that wrinkles were coming from sample preparation. Sample has been

prepared by drop casting of LLRGO dispersions onto mica and wrinkled layer was air dried [27].

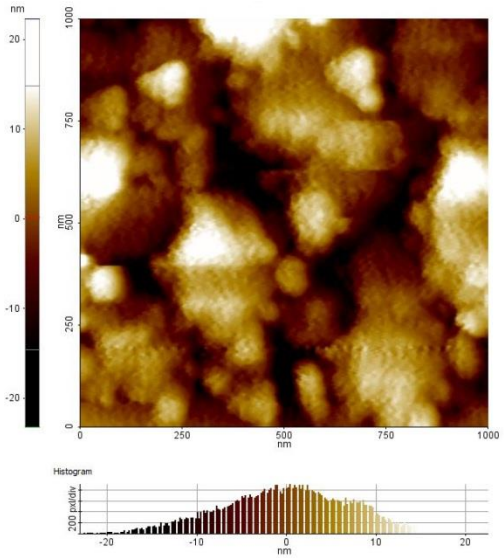

Figure 5. AFM topography of LLRGO (scan area: 1 μm × 1 μm).

3.3.2 TEM

TEM image of LLRGO in Figure 6 showed that a very thin layer with ultrathin silk veil morphology was obtained by microbial reduction process. A few layer LLRGO have a large width, around 1 μm, and transparent. TEM micrograph has also shown that layers have little wrinkles on the surface and some folds at the edges [28].

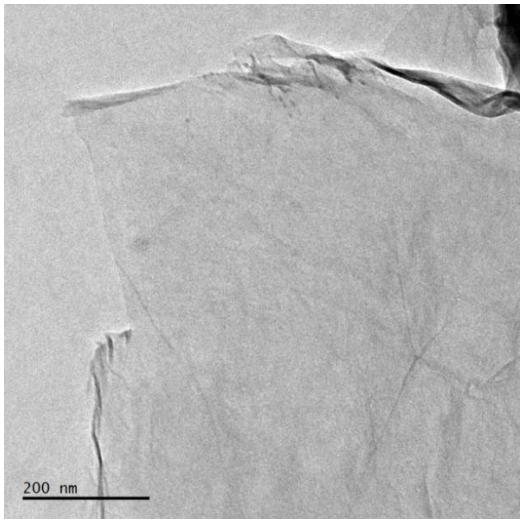

Figure 6. TEM image of LLRGO

In our previous study, *L. plantarum* were used to reduce GO and less reduction of GO was obtained with a lot of wrinkles [15]. Compared to this work, reduction with *L. lactis* has provided higher number of single layer graphene with some wrinkles. When GO and LLRGO suspensions' electrical conductivity was measured by simple multimeter, it was seen that GO has not have any resistance, however, LLRGO has 11 Ohm resistance. This small experiment showed that the reduction mechanism of *L. lactis* works very effectively in this study and has produced graphene-like structure having a potential of electrical conductivity. Further study should focus on the measurement of electrical conductivity of LLRGO.

In literature, it was reported that molecular oxygen removal of *L. lactis* from the environment is occurred by conversion either to water or peroxide. Water conversion process is either directly by water forming NADH oxidase (NoxE) or indirectly by combination of peroxide forming NADH oxidase (AhpF) and by an alkyl hydroperoxide reductase (AhpC) to convert peroxide to water. Instead of water formation, peroxide production could be obtained by superoxide dismutase (SodA) from dismutation of superoxide (O2-). These enzymes are responsible for the conversions [29]. It was also reported that peroxide accumulation under aerobic conditions was found to be non-enzymatic but followed the pyruvate pathway under high metabolic flux [30]. There are enzymatic and non-enzymatic pathways *of L. lactis* to reduce GO. This aspect is not the focus of the study. However, since, very effective reduction was observed by *L. lactis* and obtained RGO has very promising properties, the mechanism of graphene oxide reduction by *L. lactis* should be the focus of further study.

4. Conclusion

In this study, graphene oxide was successfully reduced by *L. lactis*. RGO's physical and chemical properties were determined by several instrumental methods to verify its quality compared to pristine graphene. High reduction capacity of *L. lactis* provided 1-3-layer graphene sheets with a promising electrical conductivity to be obtained. This study demonstrated that use of microorganisms is a highly suitable environmental method for graphene production. *L. lactis* could be used for reduction of GO as bioreducing agent in this method. Further studies should focus on understanding of the reduction mechanism of the *L. lactis* and the continuation of the studies to increase the electrical conductivity will contribute significantly to this area and applications on graphene.

Author's Contributions

Guldem Utkan: Drafted and wrote the manuscript, performed the experiment and result analysis.

Ethics

There are no ethical issues after the publication of this manuscript.

References

[1]. Geim, AK, Grigorieva, IV. 2013. Van der Waals heterostructures. *Nature*; 499: 419-425.

[2]. Hummers, Jr. WS, Offeman, RE., 1958. Preparation of Graphitic Oxide. *Journal of American Chemical Society*; 80(6): 1339–1339.

[3]. Aunkor, MTH, Mahbubul, IM, Saidur, R, Metselaar, HSC. 2016. The green reduction of graphene oxide. *The Royal Society of Chemistry Advances*; 6(33): 27807– 27828.

[4]. Gurunathan, S, Han, JW, Eppakayala, V, Kim, JH. 2013. Microbial reduction of graphene oxide by *Escherichia coli*: a green chemistry approach, *Colloids and Surfaces B: Biointerfaces*; 102: 772- 777.

[5]. Salas, EC, Sun, Z, Lüttge, A, Tour, JM. 2010. Reduction of graphene oxide via bacterial respiration. *American Chemical Society Nano*: 4(8): 4852– 48566.

[6]. Wang, G, Qian, F, Saltikov, CW, Jiao, Y, Li, Y. 2011. Microbial reduction of graphene oxide by Shewanella. *Nano Researc*h; 4(6): 563– 570.

[7]. Zhang, H, Yu, X, Guo, D, Qu, B, Zhang, M, Li, Q, Wang, T. 2013. Synthesis of bacteria promoted reduced graphene oxide-nickel sulfide networks for advanced supercapacitors. *American Chemical Society Applied Materials Interfaces;* 5: 7335– 7340.

[8]. Raveendran, S, Chauhan, N, Nakajima, Y, Toshiaki, H, Kurosu, S, Tanizawa, Y, Tero, R, Yoshida, Y, Hanajiri, T, Maekawa, T, Ajayan, PM, Sandhu, A, Kumar, DS. 2013. Ecofriendly route for the synthesis of highly conductive graphene using extremophiles for green electronics and bioscience. *Particles &. Particle Systems Characterizations*; 30: 573– 578.

[9]. Chen, Y, Niu, Y, Tian, T, Zhang, J, Wang, Y, Li, Y Qin, LC. 2017. Microbial reduction of graphene oxide by Azotobacter chroococcum. *Chemical Physics Letters*; 677: 143–147.

[10]. Lehner, BAE, Janssen, VAEC, Spiesz, EM, Benz, D, Brouns, SJJ, Meyer, AS, van der Zant, HSJ. 2019. Creation of Conductive Graphene Materials by Bacterial Reduction Using Shewanella Oneidensis. *ChemistryOpen*; 8: 888–895.

[11]. Fan, M, Zhu, C, Feng, ZQ, Yang, J, Liu, L, Sun, D. 2014. Preparation of N-doped graphene by reduction of graphene oxide with mixed microbial system and its haemocompatibility. *Nanoscale*; 6: 4882- 4888.

[12]. Priyadarshani Choudhary, P., Das, SK. 2019. Bio-Reduced Graphene Oxide as a Nanoscale Antimicrobial Coating for Medical Devices. *ACS Omega*; 4: 387−397.

[13]. Gurunathan, S, Han, JW, Eppakayala, V., Kim, JH. 2013. Green synthesis of graphene and its cytotoxic effects in human breast cancer cells. *Int. J. Nanomedicine*; 8: 1015–1027.

[14]. Schütz, B, Seidel, J, Sturm, G, Einsle, O, Gescher, J. 2011. Investigation of the electron transport chain to and the catalytic activity of the diheme cytochrome c peroxidase CcpA of Shewanella oneidensis. Applied Environmental Microbiology; 77: 6172– 6180.

[15]. Utkan, G, Ozturk T, Duygulu O, Tahtasakal, E, Denizci, AA. 2019. Microbial Reduction of Graphene Oxide by *Lactobacillus plantarum*. *International Journal of Nanoscience and Nanotechnology*; 15(2): 127-136 (24).

[16]. Zhou, X, Zhang, J, Wu, H, Yang, H, Zhang, J, Guo, S. 2011. Reducing graphene oxide via hydroxylamine: a simple and efficient route to graphene. *J. Phys. Chem. C*; 115(24): 11957–11961.

[17]. Zhang, J, Yang, H, Shen, G, Cheng, P, Zhang J, Guo, S. 2010. Reduction of graphene oxide via L-ascorbic acid. *Chem. Commun*.; 46(7): 1112–1114.

[18]. Wang, Y, Shi, Z, Yin, J. 2011. Facile synthesis of soluble graphene via a green reduction of graphene oxide in tea solution and its biocomposites, *ACS Appl. Mater. Interfaces*; 3(4):1127–1133.

[19]. Khanra, P, Kuila, T, Kim, NH, Bae, SH, Yu, DS, Lee, JH. 2012. Simultaneous bio-functionalization and reduction of graphene oxide by baker's yeast, *Chem. Eng. J*.; 183, :526–533.

[20]. Aunkor, M, Mahbubul, I, Saidur, R, Metselaar, HSC. 2015. Deoxygenation of graphene oxide using household baking soda as a reducing agent: a green approach. *RSC Adv*.; 5(86): 70461–70472.

[21]. Akhavan, O, Ghaderi, E. 2012. Escherichia coli bacteria reduce graphene oxide to bactericidal graphene in a self-limiting manner. Carbon; 50: 1853– 1860.

[22]. Fernandez-Merino, M, Guardia, L, Paredes, J, VillarRodil, S, Solis-Fernandez, P, Martinez-Alonso, A, Tascon, JMD. 2010. Vitamin C is an ideal substitute for hydrazine in the reduction of graphene oxide suspensions, *J. Phys. Chem. C*; 114(14): 6426–6432.

[23]. Lei, Y, Tang, Z, Liao, R, Guo, B. 2011. Hydrolysable tannin as environmentally friendly reducer and stabilizer for graphene oxide. *Green Chem*.; 13(7); 1655–1658.

[24]. Fu, C, Zhao, G, Zhang, H, Li, S. 2013. Evaluation and Characterization of Reduced Graphene Oxide Nanosheets as Anode Materials for Lithium-Ion Batteries. *Int. J. Electrochem. Sci*; 8: 6269 – 6280.

[25]. Aliyev, E, Filiz, V, Khan,, MM, Lee, YJ, Abetz, C, Abetz, V. 2019. Structural Characterization of Graphene Oxide: Surface Functional Groups and Fractionated Oxidative Debris. *Nanomaterials*; 9: 1180-1195.

[26]. Azizighannad, S, Mitra, S. 2018. Stepwise Reduction of Graphen Oxide (GO) and Its Effects on Chemical and Colloidal Properties. *Nature Scientific Reports*; 8: 10083.

[27]. Gurunathan, S, Han, Kim, JH. 2013. Green chemistry approach for the synthesis of biocompatible graphene. *Int. J. Nanomedicine*; 8: 2719-2732.

[28]. Ghosh, TK, Gope, S, Rana, D, Roy, I, Sarkar, G Sadhukhan, S, Bhattacharya, A, Pramanik, K, Chattopadhy, S, Chakraborty, M, Chattopadhyay, D. 2016. Physical and electrical characterization of reduced graphene oxide synthesized adopting green route. *Bull. Mater. Sci.*; 39 (2): 543–550.

[29]. Jiang RR, Riebel BR, Bommarius AS. 2005. Comparison of alkyl hydroperoxide reductase (AhpR) and water-forming NADH oxidase from *Lactococcus lactis* ATCC 19435. Advanced Synthesis & Catalysis; 347: 1139-1146.

[30]. van Niel EWJ, Hofvendahl K, Hahn-Hagerdal B. 2002. Formation and conversion of oxygen metabolites by *Lactococcus lactis subsp lactis* ATCC 19435 under different growth conditions. Applied and Environmental Microbiology; 68: 4350-4356.